European Journal of Chemistry

Thermal decomposition of *N*-(salicylidene)-*L*-leucine in static air atmosphere

Munusamy Vennila, Govindasamy Manikandan,
Venugopal Thanikachalam and Jayaraman Jayabharathi*

Department of Chemistry, Annamalai University, Annamalai Nagar 608 002, India

*Corresponding author at: Department of Chemistry, Annamalai University, Annamalai Nagar 608 002, India. Tel.: +91.4144.239523; fax: +91.4144.238080.
E-mail address: pvta1998@yahoo.co.in (J. Jayabharathi).*

ARTICLE INFORMATION

KEYWORDS

ABSTRACT

The thermal degradation of *N*-(salicylidene)-*L*-leucine was studied under non-isothermal conditions in air atmosphere. For kinetic analysis, the TG/DTA/DTG data obtained at three different heating rates were processed by Friedman, Kissinger-Akahira-Sunose, Flynn-Wall-Ozawa and Kissinger methods. The analysis indicates a complex reaction process which can be best described by the three dimensional (Ginstling-Brounshtein) model D4.

1. Introduction

Schiff base ligands have significant importance in chemistry. Schiff bases derived from salicylaldehyde can function as polydendate ligands and form stable complexes with transition metal ions [1-3]. Many Schiff base complexes show excellent catalytic activity in a number of reactions [4-7].

Wang *et al.* have reported *L*-α-amino acid Schiff base [8,9] which has chirality and different properties depending on the substituent. The salicylidine-amino acid Schiff bases were assembled using Cu^{2+} ion with neutral planar chelating ligand, *phen* (or *bipy*) and the chemical nuclease property of Cu-*phen* entity that intercalates into DNA groove [10] would be introduced.

Combining with the available medico radionuclide ^{64}Cu one kind of potential pharmaceutical has been investigated and found to possess antitumour activity and tumour accumulation in vivo-*R* and *S*-configuration of Cu-*phen* complexes were theoretically constructed. The geometries of the complexes were optimized using PM3 method, then ab initio B3LYP 6-31/G* calculation was performed to describe the molecular properties. The single point calculation of the three single crystals of the complexes was carried out with the theory of B3LYP 6-31/G*, the structures with and without solvents were treated separately. All calculations were carried out employing the GAUSSIAN 98 program [11].

The present article is to investigate the kinetics of thermal degradation of *N*-(salicylidene)-*L*-leucine in air atmosphere, under non-isothermal conditions. The kinetic parameters for the decomposition were calculated using Friedman, Kissinger-Akahira-Sunose (KAS), Flynn-Wall-Ozawa (FWO) and Kissinger methods.

2. Materials and methods

All the chemicals were of analytical quality and have been used without further purification. Elemental analysis (carbon, hydrogen and nitrogen) has been performed using a Heraeus Carlo Erba 1108 model at Central Drug Research Institute, Lucknow, India. FT-IR spectrum of the compound was recorded on a AVATAR model 330 using KBr pellet. Thermogravimetric analysis were carried out using a NETZSCH-Geratebare GMBH thermal analysis, STA 409 PC. The weight of the sample was constant (10 mg) for all the heating rates of 10, 15 and 20 °C/min, upto a temperature of 800 °C and air flow of 50 mL/min.

2.1. Preparation of N-(salicylidene)-L-leucine

This compound was synthesized by mixing salicylaldehyde in ethanol and sodium salt of *L*-leucine in ethanol-water (50% v/v) [12]. The mixture was heated and refluxed on a mantle for about 5 hours. The reaction mixture was cooled to room temperature and neutralized with 1:1 HCl. The colorless Schiff base was separated, filtered off, washed thoroughly with deionised water-ethanol mixture followed by ether. The product obtained was dried in a vacuum desiccator. The melting point of the compound was 114 °C (Lit. 114 °C) [12]. Anal. Calcd. for $C_{13}H_{17}NO_3$; C, 66.38; H, 7.23, N, 5.95. Found C, 66.23; H, 7.20; N, 5.85%. FT-IR (KBr disc, υ, cm^{-1}): 2958 (C-H), 1622 (C=N), (C=O), (C-N), 1073 (C-O) and 698 (C-H).

2.2. Rate equation

Usually the change in extent of reaction (α) is used to study solid state reaction kinetics

$$\alpha = \frac{m_0 - m_t}{m_0 - m_\infty} \tag{1}$$

where m_0, m_t and m_∞ are initial mass, mass at time t and mass at the end of reaction, respectively. Several reaction models [13] using $f(\alpha)$ or $g(\alpha)$ are reported in literature. Under non-isothermal conditions in which a sample is heated at a constant rate, the explicit temperature dependence of the rate equation is given by,

$$\frac{d\alpha}{dT} = \frac{A}{\beta} \exp\left(\frac{-E_a}{RT}\right) f(\alpha) \tag{2}$$

upon integration, equation (2) gives

$$g(\alpha) = \frac{A}{\beta} \int_0^T \exp\left(\frac{-E_a}{RT}\right) dT \tag{3}$$

If E_a/RT is replaced by x and integration limits transformed equation (3) becomes,

$$g(\alpha) = \frac{AE_a}{\beta R} \int_0^\infty \frac{\exp(-x)}{x^2} dx \tag{4}$$

Equation (4) can be written as

$$g(\alpha) = \frac{AE_a}{\beta R} \, p(x) \tag{5}$$

$p(x)$ has no analytical solution but has many approximations [14-16] and one of the most popular being the Coats-Redfern method [17]. This method utilizes the asymptotic series expansion for approximating the exponential integral in equation (5) giving

$$\ln\frac{g(\alpha)}{T^2} = \ln\left[\frac{AR}{\beta E_a}\left(1 - \frac{2RT}{E_a}\right)\right] - \frac{E_a}{RT} \tag{6}$$

Plotting the left hand side of equation (6), $\ln[g(\alpha)/T^2]$ *versus* $1/T$ gives E_a and A from the slope and intercept, respectively [17-26]. The model that gives the best linear fit is selected as the correct model.

2.3. Isoconversional method

According to the results of International Congress on Thermal Analysis and Calorimetry (ICTAC) kinetic project, isoconversional methods can match up to this challenge among other methods [27]. In non-isothermal kinetics, the Friedman (FR) [28], Flynn-Wall-Ozawa (FWO) [29,30] and Kissinger-Akahira-Sunose (KAS)[31-33] methods are the most popular representatives of the isoconversional methods.

2.3.1. Friedman's isoconversional method

This method [28] was one of the earliest isoconversional methods, according to which the non-isothermal rate law,

$$\beta\frac{d\alpha}{dT} = A e^{\frac{-E_a}{RT}} f(\alpha) \tag{7}$$

gives

$$\ln\left[\beta\frac{d\alpha}{dt}\right] = \ln\left[A_\alpha \, f(\alpha)\right] - \frac{E_{a,\alpha}}{RT_\alpha} \tag{8}$$

Hence, a plot of $\ln(\beta d\alpha/dT)$ *versus* $1/T$ at each α gives E_a from the slope of the plot.

2.3.2. Kissinger-Akahira-Sunose method

The Kissinger-Akahira-Sunose (KAS) method [31-33] was based on the following equation

$$\ln\frac{\beta}{T_\alpha^2} = \ln\left[\frac{AR}{E_a g(\alpha)}\right] - \frac{E_a}{RT_\alpha} \tag{9}$$

The E_a for different conversion values can be calculated from the linear plots of $\ln\left(\dfrac{\beta}{T_\alpha^2}\right)$ versus $1/T$.

2.3.3. Flynn-Wall-Ozawa method

The Flynn-Wall-Ozawa (FWO) method [29,30] was based on the following equation

$$\ln\beta = \ln\left[\frac{0.0048\,AE_a}{R g(\alpha)}\right] - 1.0516 - \frac{E_a}{RT} \tag{10}$$

for α = constant, $\ln\beta$ versus $1/T$ obtained at several heating rates yields a straight line whose slope allows evaluation of the apparent activation energy.

3. Results and discussion

Figure 1 shows TG-DTA-DTG curves corresponding to the Schiff's base. A weak endothermic effect followed by intense endothermic effect at about 285.40, 288.71 and 292.34 °C are observed at different heating rates (10, 15 and 20 K/min). The first two peaks are not accompanied by weight loss which is attributed to melting and crystal deformation of the Schiff base. The weight loss of 97.5, 98.4 and 93.0 % are observed at different heating rates. This total decomposition is accompanied by an endothermic effect with a maximum at 310 °C and the decomposition is completed after this period.

3.1. Isoconversional kinetic analysis

Friedman, KAS and FWO methods are used to determine the energy of activation (E_a) at constant several conversion degrees (α) (Table 1). The plots of $\ln(\beta d\alpha/dT)$ versus $1/T$, $\ln(\beta/T^2)$ versus $1/T$ and $\ln\beta$ *versus* $1/T$, corresponding to several conversion degrees (α) were constructed. In the present study, three different heating rates were used (10, 15 and 20 K/min). Different heating rates give different Arrhenius plots, therefore a series of E_a values can be determined from the slopes of the straight lines at conversion degrees (Table 1).

According to the Kissinger-Akahira-Sunose (KAS) isoconversional method, straight lines with the angular co-efficient -E/R were obtained and then a series of E_α values can be calculated by using equation (9).

The values of the apparent activation energies obtained by Friedman method are lower than that of KAS and FWO methods. The average values of E_a in the range $0.2 \leq \alpha \leq 0.9$ were 251.61 ± 0.58 kJ/mol (Friedman), 267.92 ± 1.91 kJ/mol (KAS) and 263.84 ± 1.90 kJ/mol (FWO) methods. The apparent activation energy sharply decreases with increase in the degree of conversion ($0.01 \leq \alpha \leq 0.2$) (Table 1; Figure 2). The data show that energy of activation independent of conversion (α), decomposed product not equilibrium with solid surface. Then, the energy of activation was found to be independent of conversion upto α = 0.94 which indicates that only one mechanism is involved for the decomposition of *N*-(salicylicdene)-*L*-leucine in air atmosphere.
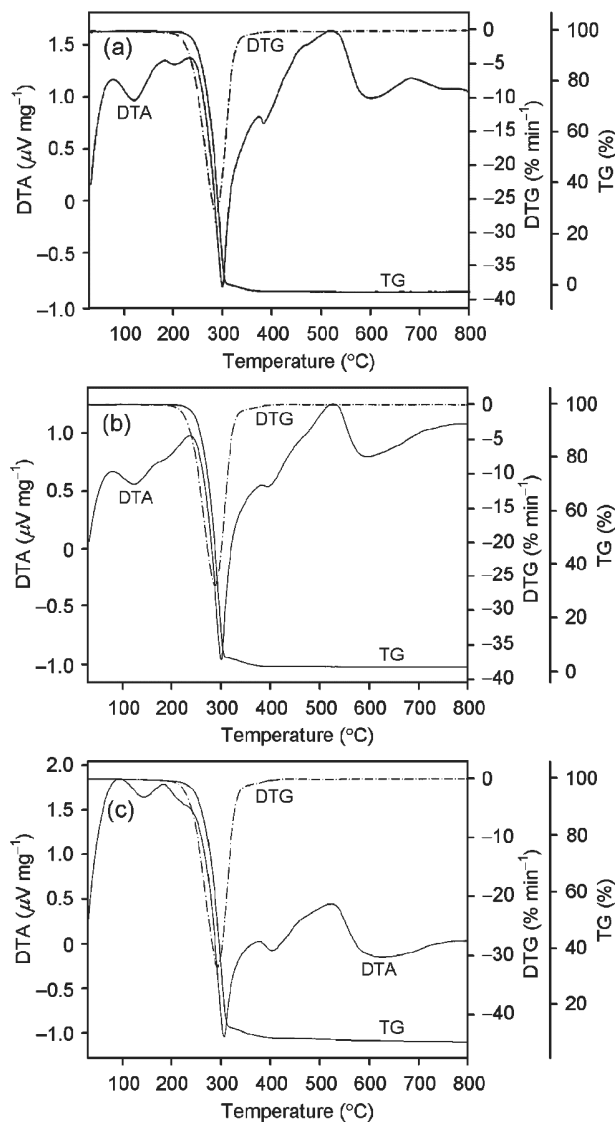
Figure 1. TG-DTG curves of *N*-(salicylidene)-*L*-leucine at different heating rates a) 10, b) 15 and c) 20 K/min in dynamic air atmosphere.
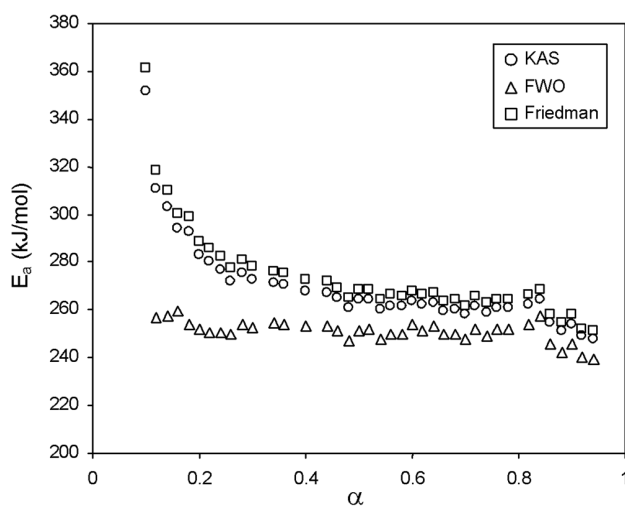

Figure 2. Isoconversional activation energy corresponding to the linear non-isothermal decomposition in dynamic air atmosphere of the *N*-(salicylidene)-*L*-leucine .

Table 1. Temperatures corresponding to the same degree of conversion at different heating rates for *N*-(salicylidene)-*L*-leucine.

| α	Heating Rates			E_a (kJ/mol)		
	10K	15K	20K	Friedman method	KAS method	FWO method
0.10	524.28	526.44	528.60	-	361.02	351.57
0.12	528.20	530.45	533.13	257.06	318.06	310.79
0.14	529.60	531.75	534.64	257.23	310.15	303.29
0.16	532.80	535.24	538.11	259.37	300.25	293.94
0.18	532.80	535.93	538.17	254.12	298.80	292.55
0.20	535.60	538.20	541.18	252.11	288.94	283.23
0.22	537.40	540.78	543.10	250.54	285.70	280.18
0.24	539.30	542.50	545.13	250.70	282.25	276.93
0.26	541.40	543.34	547.07	249.95	277.31	272.26
0.28	542.60	545.90	548.53	254.24	280.76	275.56
0.30	544.10	547.20	550.12	252.93	277.89	272.86
0.34	546.60	549.30	552.64	254.48	276.47	271.55
0.36	547.70	550.43	553.79	254.11	275.35	270.51
0.40	550.30	552.90	556.46	253.17	272.71	268.03
0.44	552.00	554.91	558.28	253.31	272.05	267.43
0.46	553.20	556.02	559.54	250.98	269.36	264.90
0.48	554.60	557.20	560.99	247.30	265.37	261.13
0.50	555.35	558.16	561.75	251.30	268.52	264.13
0.52	556.20	558.88	562.58	252.03	268.66	264.28
0.54	557.20	559.95	563.71	247.44	264.34	260.18
0.56	557.90	560.79	564.42	249.85	266.17	261.94
0.58	559.30	561.81	565.75	250.12	265.61	261.43
0.60	560.40	562.51	566.66	253.76	268.12	263.84
0.62	560.70	563.52	567.26	251.28	266.24	262.05
0.64	561.80	564.24	568.24	253.14	267.27	263.04
0.66	563.20	565.10	569.50	249.59	263.47	259.46
0.68	563.50	566.00	570.06	250.16	264.13	260.09
0.70	564.20	566.80	570.86	247.65	261.76	257.84
0.72	564.53	567.58	571.24	251.81	265.52	261.43
0.74	565.00	568.18	571.80	249.17	263.11	259.15
0.76	566.20	569.00	572.90	251.64	264.73	260.71
0.78	567.60	570.50	574.36	251.86	264.58	260.58
0.82	569.00	571.78	575.72	254.16	266.19	262.13
0.84	570.00	572.61	576.63	257.49	268.82	264.65
0.86	570.80	573.67	577.76	245.79	258.33	254.69
0.88	571.60	574.52	578.67	242.26	254.99	251.53
0.90	572.60	575.35	579.57	245.83	257.87	254.28
0.92	574.10	576.65	581.16	239.85	252.09	248.81
0.94	575.90	577.87	582.74	239.44	251.13	247.93

3.2. Invariant kinetic parameters (IKP) method

The kinetics parameters are calculated using equation (6) and values are listed in Table 2. Lesnikovich and Levchik [34] suggested that correlating these values by the apparent compensation effect, $\ln A = a_\beta + b_\beta E_a$, one obtains the compensation effect parameters, a_β and b_β, which strongly depends on the heating rates (β) as well as on the considered set of conversion functions. The straight lines $\ln A$ versus E_a for three constant heating rates should intersect at a point (isoparametric point [35]) which corresponds to the true values of the activation energy and pre-exponential factor. These were named as invariant kinetic parameters. Invariant kinetic parameters E_{inv} and A_{inv} are determined according to literature method, using various combination models and listed in Tables 3 and 4 (Figure 3). The E_a calculated by Friedman method coincided with AKM (all kinetic models).

By introducing the reaction model, $g(\alpha) = \left(1 - \dfrac{2}{3}\alpha\right) - (1-\alpha)^{2/3}$ in to equation (5), equation (11) is obtained

$$\left(1 - \frac{2}{3}\alpha\right) - (1-\alpha)^{2/3} = \frac{AE_a p(x)}{R\beta} \qquad (11)$$

The plot of $\left(1 - \dfrac{2}{3}\alpha\right) - (1-\alpha)^{2/3}$ against $\dfrac{E_a p(x)}{R\beta}$ at the different (Figure 3) heating rates is considered. By using equation (11), the A value was determined from the slope of the line shown in Figure 4.
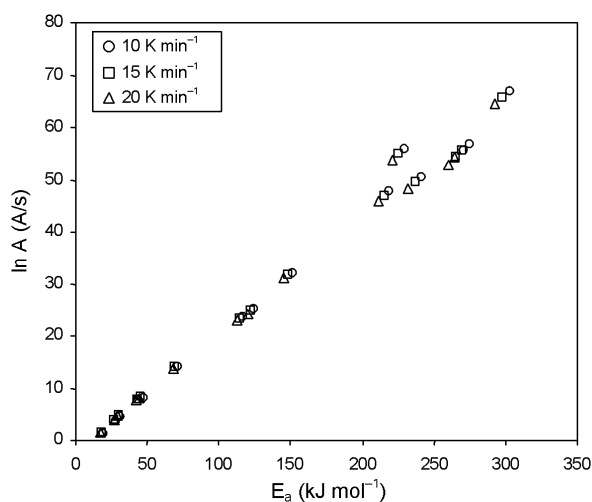
Figure 3. Kinetic compensation effect for the decomposition of *N*-(salicylidene)-*L*-leucine in static air atmosphere.

By applying the three-dimensional diffusion controlled (Ginstling-Brounshtein) D4 model $E_a = 251.61 \pm 0.58$ kJ/mol, the pre-exponential (frequency) factor $A = 1.29 \times 10^{22}$ 1/min ($\ln A = 50.91$). The obtained value of $\ln A$ is in good agreement with that from the invariant method ($\ln A = 53.20$).

Therefore, the corresponding kinetic equation for describing the non-isothermal decomposition process of *N*-(salicylidene)-*L*-leucine is given by

Table 2. Arrhenius parameters for non-isothermal decomposition of *N*-(salicylidene)-*L*-leucine obtained from model fitting method.

Kinetic model	β = 10 K/min			β = 15 K/min			β = 20 K/min		
	E_a (kJ/mol)	ln A (A/s)	r	E_a (kJ/mol)	ln A (A/s)	r	E_a (kJ/mol)	ln A (A/s)	r
P2	47.16	8.17	-0.995	46.03	8.23	-0.995	44.90	8.17	-0.994
P3	28.36	3.71	-0.994	27.58	3.86	-0.994	26.81	3.91	-0.992
P4	19.01	1.34	-0.992	18.42	1.55	-0.992	17.82	1.63	-0.990
F1	151.23	31.98	-0.998	148.25	31.50	-0.998	145.26	30.90	-0.998
F2	219.14	47.65	-0.981	215.10	46.84	-0.981	211.01	45.91	-0.981
F3	303.73	66.99	-0.958	298.38	65.78	-0.958	292.93	64.44	-0.958
D1	229.56	55.74	-0.996	225.15	54.84	-0.996	220.76	53.85	-0.996
D2	241.96	50.52	-0.999	237.19	49.52	-0.999	232.42	48.41	-0.999
D3	275.50	56.71	-1.000	270.18	55.54	-1.000	264.86	54.27	-1.000
D4	270.98	55.43	-0.998	265.50	54.23	-0.998	260.04	52.93	-0.998
A2	71.05	13.98	-0.998	69.53	13.92	-0.998	68.00	13.75	-0.998
A3	43.85	7.65	-0.998	42.83	7.74	-0.998	41.80	7.71	-0.998
A4	30.96	4.53	-0.997	30.17	4.68	-0.997	29.37	4.72	-0.998
R2	124.89	25.15	-1.000	122.34	24.79	-1.000	119.78	24.32	-1.000
R3	117.53	23.70	-0.999	115.10	23.38	-0.999	112.66	22.95	-0.999

Table 3. Compensation effect parameters for several combinations of kinetic models for *N*-(salicylidene)-*L*-leucine.

β (K/min)	AKM			AKM–{D1; D3; D4}		
	a_β, A/s	b_β/mol/J	r	a_β, A/s	b_β/mol/J	r
10	-1.72733	0.22207	0.995	-2.61283	0.22641	0.999
15	-1.97715	0.22332	0.995	-2.24555	0.2252	0.995
20	-2.34321	0.22456	0.995	-1.99356	0.22391	0.999
β (K/min)	AKM–{F2; D1; D2; D3; D4}			AKM - {P4; F2; D1; D3; D4; A1; A2}		
	a_β, A/s	b_β/mol/J	r	a_β, A/s	b_β/mol/J	r
10	-2.73824	0.22882	0.999	-2.81444	0.22914	0.999
15	-2.36953	0.22765	0.999	-2.44544	0.22791	0.999
20	-2.11633	0.22646	0.999	-2.18782	0.22676	0.999

Table 4. IKP for several combinations of kinetic models for *N*-(salicylidene)-*L*-leucine.

Kinetic model	E_{inv} (kJ/mol)	ln A_{inv}	-r
AKM	247.27	53.20	0.994
AKM - {D1; D3; D4}	244.13	53.36	0.992
AKM - {F2; D1; D2; D3; D4}	263.37	57.55	0.993
AKM - {P4; F2; D1; D3; A1; A2}	262.99	57.47	0.993

$$\beta \frac{d\alpha}{dT} = 1.29 x 10^{22}. \exp\left(\frac{-251.61}{RT}\right) 3/2\left[(1-\alpha)^{-1/3} - 1\right] \qquad (12)$$

where $3/2\left[(1-\alpha)^{-1/3} - 1\right]$ represents the differential form of three dimensional diffusion (D4) controlled reaction. However this is further conformed by masterplot method (Figure 5). The overall masterplot of the compound shown in Figure 6.

Figure 5. Theoretical and experimental master plots of *N*-(salicylidene)-*L*-leucine at 10 K heating rate (non-isothermal).
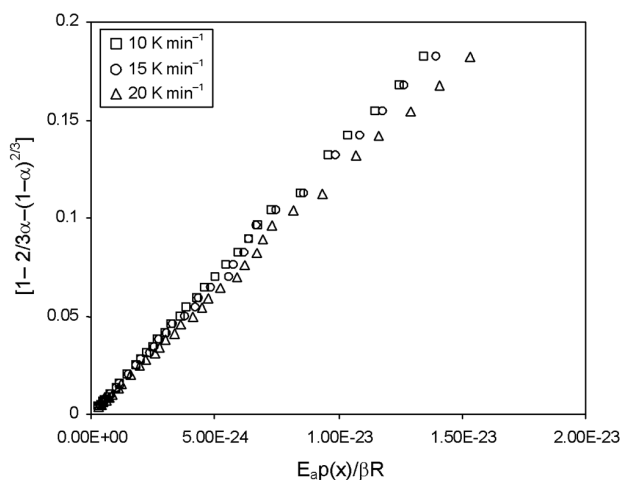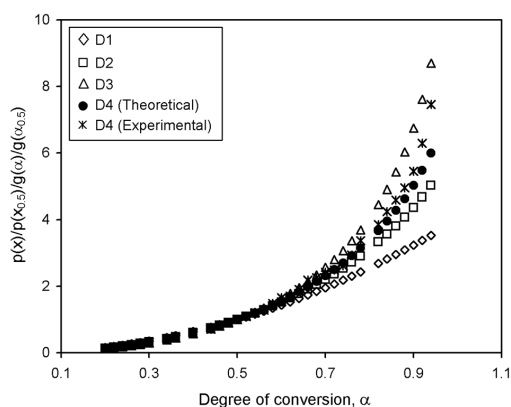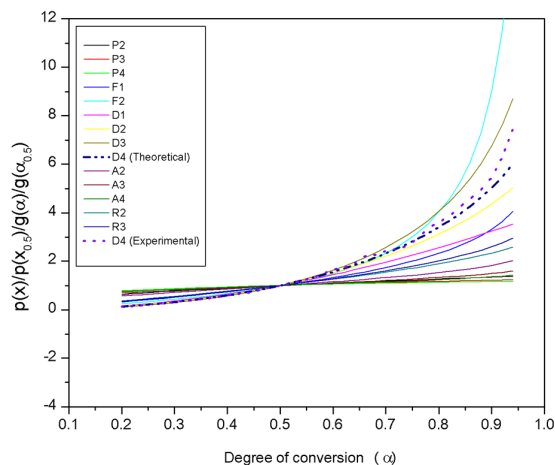
Figure 4. Plots of $[1-2/3\alpha-(1-\alpha)^{2/3}]$ against $E_a p(x)/\beta R$ for the decomposition of *N*-(salicylidene)-*L*-leucine at heating rates of 10, 15 and 20 K/min.

Figure 6. The overall theoretical and experimental masterplots of *N*-(salicylidene)-*L*-leucine at 10 K heating rate (non-isothermal).

Table 5. Determination of kinetic parameters by Kissinger method.

Peak Temperature (K)	E_a (kJ/mol)	ln A (A/s)	r	$\Delta G^{\neq}$ (kJ/mol)	$\Delta H^{\neq}$ (kJ/mol)	$\Delta S^{\neq}$ (J/mol.K)
558.40						
561.71	242.31	52.02	0.9914	135.15	237.4	-182.57
565.34						

The activation energy and pre-exponential factor are also calculated by Kissinger single point method [31] and the thermodynamic parameters of activation can be calculated [36-39] and data are listed in Table 5.

$$A \exp(-E_a/RT_p) = \upsilon \exp(-\Delta G^{\neq}/RT_p) \qquad (13)$$

$$\Delta H^{\neq} = E_a - RT_p \qquad (14)$$

$$\Delta G^{\neq} = \Delta H_p^{\neq} - T_p \Delta S^{\neq} \qquad (15)$$

where $\Delta G^{\neq}$ is the Gibbs free energy of activation, $\Delta H^{\neq}$ the enthalpy of activation, $\Delta S^{\neq}$ the entropy of activation and υ the Einstein vibrational frequency, $\upsilon = k_B T/h$ (where k_B and h are Boltzmann and Planck's constants, respectively).

The values are calculated at the peak temperature T_p in the DTG curve for the corresponding stage.

Table 5 reveals that the value of $\Delta S^{\neq}$ is negative. It means that the activated complexes have greater degree of arrangement than the initial stage. In terms of the theory of activated complex [36-39], the thermal decomposition of *N*-(salicylidine)-*L*-leucine may be interpreted as slow. This was confirmed by the very high value of activation energy (E_a = 242.31 kJ/mol). The positive values of $\Delta H^{\neq}$ and $\Delta G^{\neq}$ showed that the processes in highly endothermic and is non-spontaneous.

4. Conclusion

The thermal decomposition of *N*-(salicylididene)-*L*-leucine was investigated in detail by TG, DTA and DTG. The process involved melting, solid-solid phase transition and decomposition. The kinetic parameters of decomposition were obtained by the isoconversional and invariant methods. The decomposition reaction is endothermic as shown by the positive value of $\Delta G^{\neq}$. The three dimensional model D4 can be the most probable model which can give adequate kinetic description for the thermal decomposition of the compound chosen for study.

Acknowledgement

References

[1]. Nejati, K.; Rezvani. Z.; Massoumi, B. *Dyes and Pigments* **2007**, *75*, 653-657.
[2]. Souza, P.; Garcia-Vazqueez, J. A.; Masaquer, J. R. *Transit. Metal Chem.* **1985**, *10*, 410-412.
[3]. Naeimi, H.; Safari, J.; Heidarzezhad, A. *Dyes and Pigments* **2007**, *73*, 251-253.
[4]. Lippard, S. S.; Berg, J. M.; Principles of Bioinorganic Chemistry, California, University Science Books, 1994.
[5]. Tumer, M.; Ekiria, D.; Tumer, F.; Bulur, A. *Spectrochim. Acta A* **2007**, *67*, 916-929.
[6]. Puri, A.; Berden, I.; Morgenstem-Badarasu; Gref, A.; Perrae-Fluvet, M. *Inorg. Chim. Acta* **2001**, *320*, 167-171.
[7]. Ispin, E. *Dyes and Pigments* **2009**, *82*, 13-19.
[8]. Wang, M. Z.; Meng, Z. X.; Liu, Bo. Li.; Cai, G. L.; Zhang, C. L.; Wang, X. Y. *Inorg. Chem. Commun.* **2005**, *8*, 368-371.
[9]. Guirard, B. M.; Snell, E. E.; In: Florkin, M.; Stotz, E. H. (Eds.) Comprehensive Biochemistry, Elsevier, Amsterdam, 1981.
[10]. Sigman, D. S.; Mazumter, A.; Perrin, D. M.; *Chem. Rev.* **1993,** *93*, 2295-2316.
[11]. Gaussian 98, Gaussian, Inc., Pittsburgh PA, 1998.
[12]. Howard, E. S.; Elizabeth, P.; Burrows, Maurice, J.; Marks, Robert, D.; Lynch, Chen, F. M. *J. Am. Chem. Soc.* **1977**, *99*, 707-713.
[13]. Khawam, A.; Flangan, D. R. *Thermochim. Acta* **2005**, *436*, 101-112.
[14]. Chen, H. J.; Lai, K. M. *J. Chem. Eng.* Japan **2004**, *37(a)*, 1172-1178.
[15]. Doyle, C. D. *J. Appl. Polym. Sci.* **1961**, *5*, 285-292.
[16]. Agarwal, R. K.; Sivasubramanian, M. S. *Aiche. J.* **1987**, *33*, 1212-1214.
[17]. Coats, A. W.; Redfern, J. P. *Nature* (London) **1964**, *201*, 68-69.
[18]. Ahmaruzzamam, M.; Sharma, D. K. *J. Anal. Appl. Pyrol.* **2005**, *73*, 263-275.
[19]. Perez-Maqueda, L. A.; Sanchez-Jimenez, P. E.; Criado, J. M. *Polymer* **2005**, *46*, 2950-2954.
[20]. Barral, L.; Difz, F. J.; Garcia-Garbal, S.; Lopez, J.; Montero, B.; Montes, R.; Ramirez, C.; Rico, M. *Eur. Poly. J.* **2005**, *41*, 1662-1666.
[21]. Slovak, V.; Susak, P. *J. Anal. Appl. Pyrolysis* **2004**, *72*, 249-252.
[22]. Vlaev, L. T.; Markoversuska, G.; Lyubchev, L. A. *Thermochim. Acta* **2003**, *406*, 1-7.
[23]. Srikanth, S.; Chakravortty, M. *Thermochim. Acta* **2001**, *370*, 141-148.
[24]. Ei-Hm, D.; Gabal, M. A.; El-Bellihi, A. A.; Eissa, N. A.; *Thermochim. Acta* **2001**, *376*, 43-50.
[25]. Joseph, K.; Sridharan, R.; Gnanasekaran, T. *J. Nucl. Mater.* **2000**, *281*, 129-139.
[26]. Hu, H.; Chen, Q.; Yin, Z.; Zhang, P.; Zou, J.; Che, H. *Thermochim. Acta* **2002**, *389*, 79-83.
[27]. Huang, J. W.; Chang, C. C.; Kang, C. C.; Yeh, M. Y. *Thermochim. Acta* **2008**, *468*, 66-74.
[28]. Friedman, H. L. *J. Polym. Sci. Polym. Lett.* **1963**, *6C*, 183-195.
[29]. Flynn, J. H.; Wall, L. A. *J. Res. Nat. Bur. Stand.* **1966,** *70A*, 487-523.
[30]. Ozawa, T. *Bull. Chem. Soc. Jpn.* **1965**, *38*, 1881-1886.
[31]. Kissinger, H. E. *Anal. Chem.* **1957**, *29*, 1702-1706.
[32]. Kissinger, H. E. *J. Res. Nat. Bur. Stand.* **1956**, *57*, 217-221.
[33]. Akahira, T.; Sunose, T.; *Res. Report CHIBA Inst. Technol.* **1971**, *16*, 22-31.
[34]. Lesnikovich, A. I.; Levchik, S. V. *J. Therm. Anal. Calorim.* **1983**, *27*, 89-93.
[35]. Lesnikovich, A. I.; Levchik, S. V. *J. Therm. Anal. Calorim.* **1985**, *30*, 237-262.
[36]. Bamford, C. H.; Tipper, C. F. H. (Eds.) Comprehensive chemical kinetics, Vol. 22, Reactions in the solid state, Elsevier Sci. Publ. Comp. Amsterdam, 1980.
[37]. Cordes, H. F. *J. Phys. Chem.* **1968**, *72*, 2185-2189.
[38]. Criado, J. M.; Perez-Maqueda, L. A.; Sanchez-Jimenez, P. E. *J. Therm. Anal. Calorim.* **2005**, *82*, 671-675.
[39]. Sokolskii, D. A.; Druz, V. A. Introduction in theory heterogenous catalysis, Vyshaya Shkola, Moscow, 1981 (in Russian).